Fabrication and characterization of on-chip optical nonlinear chalcogenide nanofiber devices

Qiming Zhang,[1] Ming Li,[1] Qiang Hao,[2] Dinghuan Deng,[3] Hui Zhou,[2] Heping Zeng,[2] Li Zhan,[3] Xiang Wu,[1] Liying Liu,[1] and Lei Xu[1,*]

[1]*Key Lab for Micro and Nanophotonic Structures (Ministry of Education), Department of Optical Science and Engineering, School of Information Science and Engineering, Fudan University, Shanghai 200433, China*

[2]*State Key Laboratory of Precision Spectroscopy, East China Normal University, Shanghai 200062, China*

[3]*Institute of Optics and Photonics, Department of Physics, State Key Lab of Advanced Optical Communication Systems and Networks, Shanghai Jiao Tong University, Shanghai 200240, China*

**Corresponding author: leixu@fudan.ac.cn*

Received September 23, 2010; accepted October 16, 2010;
posted October 26, 2010 (Doc. ID 135544); published November 11, 2010

Chalcogenide (As_2S_3) nanofibers as narrow as 200 nm in diameter are drawn by the fiber pulling method, are successfully embedded in SU8 polymer, and form on-chip waveguides and high-Q microknot resonators ($Q = 3.9 \times 10^4$) with smooth cleaved end faces. Resonance tuning of resonators is realized by localized laser irradiation. Strong supercontinuum generation with a bandwidth of 500 nm is achieved in a 7-cm-long on-chip chalcogenide waveguide. Our result provides a method for the development of compact, high-optical-quality, and robust photonic devices.

OCIS codes: 060.4370, 140.3948.

Subwavelength fibers and nanofibers directly drawn from optical fibers have attracted much attentions owing to their low optical loss, high uniformity, and surface smoothness compared with electron beam lithography, laser ablation, and the template-based method [1]. These unique advantages brought from direct drawing widely expanded the application of nanofibers into the fields of communications, nonlinear optics, sensing, lasers, biology, and chemistry [2]. One key problem of nanofibers for these applications is the degradation of optical properties over time when bare fibers are stored in air. Another problem is the lack of robustness if nanofibers are not fixed. The solution to these problems is the assembling of nanofibers on a solid substrate to increase their stability over time. Although low refractive index materials, such as aerogels and Teflon [3,4], have been applied to embed silica-based nanofibers, the refractive index difference between the core and cladding is low, which changes the high confinement properties of nanofibers. An alternative method is making nanofibers with higher refractive index materials, such as tellurite glasses and chalcogenide glasses [5,6]. Among these glasses, chalcogenide glasses have gained extensive interests, not only because of their high refractive index, wide transparent window, and ultrahigh third-order optical nonlinearity, but also their rich physicochemical properties, such as photoinduced phase change and photopolymerization, upon light exposure [7]. Low-threshold optical nonlinear phenomenon (supercontinuum generation) has been demonstrated in chalcogenide nanofibers due to the high optical nonlinearity of the material and strong optical confinement of the structure [6,8]. In this Letter, we report the fabrication and characterization of on-chip chalcogenide subwavelength fibers, which combine the good optical quality of nanofibers and robustness of the on-chip devices. Low-loss on-chip waveguides were successfully realized. Also on-chip high-Q chalcogenide microknot resonators and supercontinuum generation were demonstrated.

The chalcogenide fiber for drawing is a step-index multimode commercial fiber (Toptic Fiber, Inc., Beijing, China). The outer diameter of the fiber is 100 μm. The core/cladding ratio is 5:6, and the molar ratios of the As:S are 38:62 and 35:65 for core and cladding, respectively. The nanofibers were tapered down by hand. The narrowest fiber obtained was 200 nm in diameter [Fig. 1(a)] when one end attached to the heater (the heating temperature is about 180 °C) and another end was pulled by hand. As far as we know, this is the narrowest chalcogenide nanofibers that have ever been reported.

The chalcogenide fibers were then fixed on silicon wafers to form on-chip devices. The wafer has a 2-μm-thick thermally oxidized SiO_2 layer, which served as the buffer layer. The on-chip device fabrication process is as follows. First, a thin layer of SU8 was spin coated on a silicon wafer. Two ends of the chalcogenide fiber were mounted and aligned to the wafer by two translational stages. Second, the chalcogenide fiber was fixed on the SU8. Another layer of SU8 was spin coated to cover the fiber. The SU8 is a very robust polymer and can be fully cured at a temperature less than the glass transition temperature of As_2S_3 (180 °C). Moreover, because the fiber is tightly bound by the SU8, the whole chip can be cleaved by dicing the silicon wafer. The cleaved end face of the chip was analyzed by a scanning electron

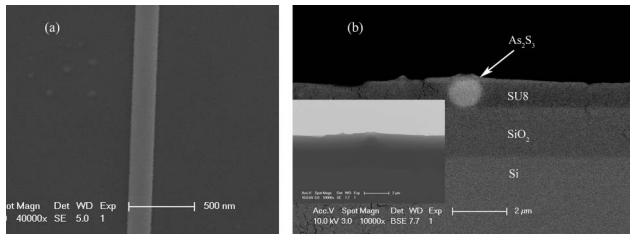

Fig. 1. (a) SEM image of the chalcogenide fiber in a diameter of 200 nm. (b) BE image of on-chip chalcogenide fiber facet after cleavage; the inset shows the SE image of on-chip fiber facet after cleavage.

microscope (SEM). A backscattering electron (BE) image and a secondary electron (SE) image of the same surface are shown in Fig. 1(b). The SE image reveals the surface morphology is flat and smooth, while the BE image, which is sensitive to the atomic weight of the elements or the density of material, clearly illustrates that the As_2S_3 is well embedded in SU8. Thus, a low coupling loss is expected.

Because the end face is flat and highly reflective, the propagation loss of the on-chip subwavelength chalcogenide fibers can be measured by Fabry–Perot interference between the reflections of two end faces [9]. The light was focused into the fibers through a lensed fiber with a focusing spot diameter of about 5 μm. Fibers in a diameter of 1 and 0.6 μm have optical loss of 1.1 ± 0.1 dB/cm and 2.5 ± 0.3 dB/cm, respectively, and the insertion loss is about 24 ± 2 dB and 42 ± 2 dB, respectively. The insertion loss is large owing to the coupling loss, which originates from the mode mismatch between the chalcogenide fiber and the lensed fiber. We believe that the insertion loss can be further reduced by using tapered fiber structures in the input end [10] or using a lensed fiber with a smaller focal spot diameter.

One important application of the nanofibers is forming high-Q resonators by simply knotting the fiber. However, the temporal stability of the knots is a problem if the resonator is not fixed [11]. By embedding the microknots in SU8 on a silicon wafer, the resonator becomes very robust. Figure 2(a) shows the optical image of the microknot fabricated from a 2 μm diameter fiber. The ring diameter is about 600 μm. The transmission spectrum of the microknot shows a periodic structure with a free spectral range of 0.573 nm and an FWHM of $\Delta\lambda = 0.040$ nm at a wavelength of $\lambda = 1550$ nm [see Fig. 2(b)], which corresponds to a cavity Q factor of $Q = \lambda/\Delta\lambda = 3.9 \times 10^4$. The Q factor obtained from these microknots is close to other reports of silica knots (5×10^4) [11] and higher than the chalcogenide–silica hybrid reef knots (1×10^4) [12].

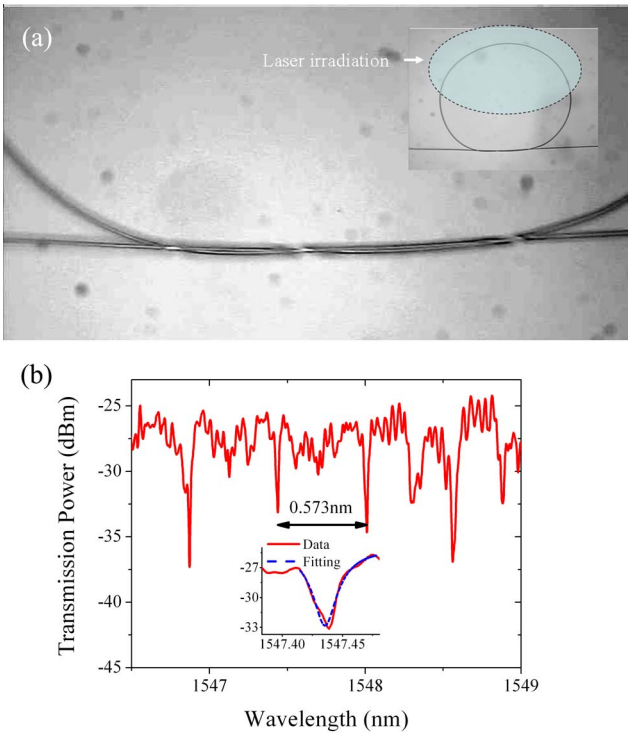

Fig. 2. (Color online) (a) Optical reflective image of the intertwisted overlap region of chalcogenide microknots in a diameter of 600 μm; the inset shows the optical reflective image of the complete microknots. (b) Transmission spectrum of the microknots; the inset shows the result and the Lorentizan fitting of a single resonant peak.

Chalcogenide glasses are highly photosensitive; its refractive index can be tuned by laser irradiation. Thus, the resonant wavelength of a fabricated chalcogenide microknot can be easily post-tuned. To demonstrate post-tuning, part of the microknots were irradiated by a cw laser in a wavelength of 532 nm at an intensity of 63 mW/cm^2. The laser was focused in the shadowed region indicated in the inset of Fig. 2(a) to avoid change in the coupling coefficient induced by the refractive index change in the knotting region. The resulting peak shift was monitored in real time. The inset of Fig. 3 shows the peak shift in the first few minutes. The resonant peak shifts to a shorter wavelength, which indicates a negative refractive index change induced by the laser. Figure 3 shows that the peak shift increases as a function of exposure time. The result can be fitted by a single-exponential decay curve. Refractive index change (Δn) can be calculated by $\Delta n = n_e \times \Delta\lambda/\lambda$. ($\Delta\lambda$ stands for the wavelength shift; n_e is the effective refractive index of the cavity.) Finite-element-method simulations give n_e equal to 2.38. The largest peak shift is about 1.5 nm, which corresponds to a refractive index change of -2.4×10^{-3}.

Optical nonlinearity is one important application field for chalcogenide glasses. To demonstrate the potential of our subwavelength on-chip fibers as nonlinear optical devices, we measured the supercontinuum generation in the fibers. A 125 fs 54 MHz mode-locked fiber laser [13] at 1560 nm was launched into the subwavelength fibers through a lensed fiber with a focal spot size of 5 μm. Output spectra were collected by a multimode fiber into an optical spectrum analyzer (OSA). 7-cm-long chalcogenide fibers in different diameters (0.5 to 2 μm) were used in the experiment. Figure 4 shows the strong transmitted light spectrum broadening after passing a 1 μm

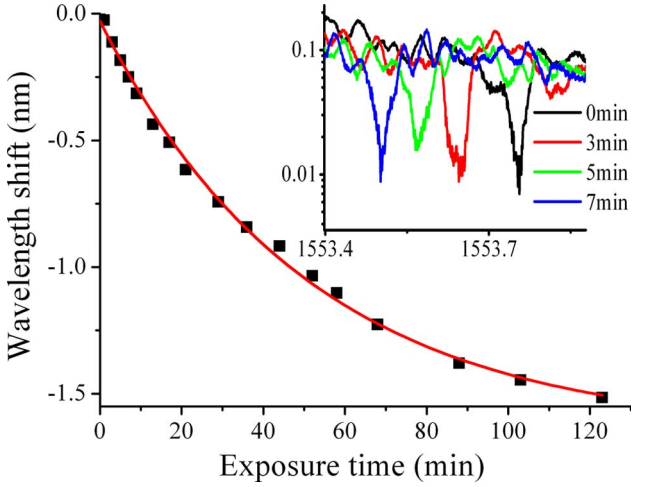

Fig. 3. (Color online) Peak shift as a function of exposure time. Black dots are experimental data, and the solid curve is an exponential decay fitting. The inset shows the transmission spectra of the microknots during irradiation by a 532 nm laser.

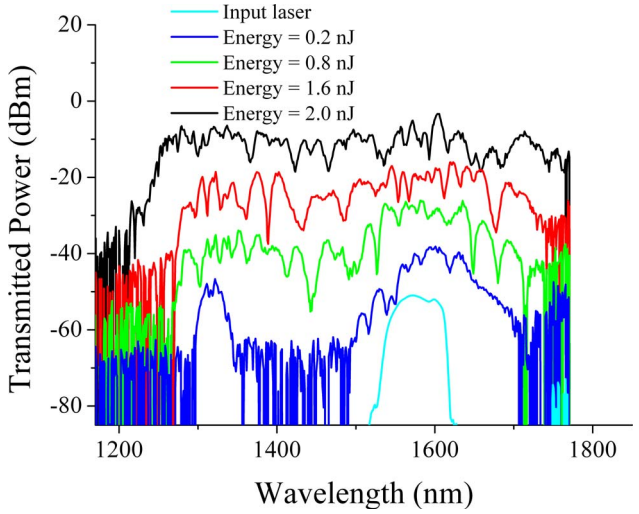

Fig. 4. (Color online) Transmission spectra of a 1560 nm femtosecond laser after passing a 7-cm-long 1 μm diameter on-chip chalcogenide waveguide.

diameter fiber. Supercontinuum covers a wavelength range 1200–1700 nm at an input pulse energy of 2 nJ (peak power: 16 kW). The long wavelength limit comes from the OSA response limit. Supercontinuum occurs when dispersion of the device is zero. As_2S_3 glass has large normal material dispersion ($D = -360$ ps/nm/km) at 1550 nm [14]; however, waveguide geometry dispersion can compensate the material dispersion [15]. Therefore, chalcogenide fiber in a size of 1 μm has almost zero total dispersion at around 1550 nm and is most suitable for effective supercontinuum generation. The relatively higher (2000 times) peak power than the other report on the As_2Se_3 nanofiber (7.8 W) [6] is related to about four times lower in third-order nonlinearity of As_2S_3 than As_2Se_3 and insertion loss of about 24 ± 2 dB. In future experimental work, the input coupling coefficient can be increased to further lower the threshold power. On the other hand, owing to the wide transparent window of As_2S_3 in IR, this structure can be used as on-chip mid-IR supercontinuum sources up to 6 μm by optimizing core sizes.

In summary, we demonstrated that on-chip subwavelength chalcogenide fibers can form various types of functional devices with robust and excellent optical properties. Supercontinuum as broad as 500 nm was demonstrated in a dispersion-engineered chalcogenide fiber device. With the wide transparent window and group velocity dispersion that is largely variable, on-chip subwavelength chalcogenide fibers can be foreseen as a compact, high-optical-quality, and robust broadband nonlinear devices.

This work is supported in part by the National Natural Science Foundation of China (NSFC) (grants 60638010, 10874033, 60907011, 61078052, and 11074051) and the Shanghai Science and Technology Commission (SCST) (grant 08XD14006).

References

1. L. M. Tong, R. R. Gattass, J. B. Ashcom, S. L. He, J. Y. Lou, M. Y. Shen, I. Maxwell, and E. Mazur, Nature **426**, 816 (2003).
2. G. Brambilla, F. Xu, P. Horak, Y. Jung, F. Koizumi, N. P. Sessions, E. Koukharenko, X. Feng, G. S. Murugan, J. S. Wilkinson, and D. J. Richardson, Adv. Opt. Photon. **1**, 107 (2009).
3. L. M. Tong, J. Y. Lou, R. R. Gattass, S. L. He, X. Chen, L. Liu, and E. Mazur, Nano Lett. **5**, 259 (2005).
4. F. Xu and G. Brambilla, Opt. Lett. **32**, 2164 (2007).
5. L. M. Tong, L. L. Hu, J. J. Zhang, J. R. Qiu, Q. Yang, J. Y. Luo, Y. H. Shen, J. L. He, and Z. Z. Ye, Opt. Express **14**, 82 (2006).
6. D. Yeom, E. C. Mägi, M. R. E. Lamont, M. A. F. Roelens, L. Fu, and B. J. Eggleton, Opt. Lett. **33**, 660 (2008).
7. A. Zakery and S. R. Elliott, J. Non-Cryst. Solids **330**, 1 (2003).
8. M. Liao, C. Chaudhari, G. Qin, X. Yan, C. Kito, T. Suzuki, Y. Ohishi, M. Matsumoto, and T. Misumi, Opt. Express **17**, 21608 (2009).
9. R. G. Walker, Electron. Lett. **21**, 581 (1985).
10. V. R. Almeida, R. R. Panepucci, and M. Lipson, Opt. Lett. **28**, 1302 (2003).
11. X. S. Jiang, L. M. Tong, G. Vienne, X. Guo, A. Tsao, Q. Yang, and D. Yang, Appl. Phys. Lett. **88**, 223501 (2006).
12. G. Vienne, A. Coillet, P. Grelu, M. E. Amraoui, J. Jules, F. Smektala, and L. M. Tong, Opt. Express **17**, 6224 (2009).
13. D. H. Deng, L. Zhan, Z. C. Gu, Y. Gu, and Y. X. Xia, Opt. Express **17**, 4284 (2009).
14. F. Luan, M. D. Pelusi, M. R. E. Lamont, D. Y. Choi, S. Madden, B. Luther-Davies, and B. J. Eggleton, Opt. Express **17**, 3514 (2009).
15. L. M. Tong, Z. Y. Lou, and E. Mazur, Opt. Express **12**, 1025 (2004).